Available online at www.sciencedirect.com
SCIENCE DIRECT®
ACADEMIC PRESS
Journal of Sound and Vibration 267 (2003) 1065–1084
JOURNAL OF SOUND AND VIBRATION
www.elsevier.com/locate/jsvi

A method to determine dynamic loads on spur gear teeth and on bearings

L. Vedmar*, A. Andersson

Department of Machine Elements, Lund Institute of Technology, P.O. Box 118, Lund, SE-221 00, Sweden

Received 8 July 2002; accepted 29 October 2002

Abstract

A method is described which can be used to calculate dynamic gear tooth force and bearing forces. The model includes elastic bearings. The gear mesh stiffness and the path of contact are determined using the deformations of the gears and the bearings. This gives contact outside the plane-of-action and a time-varying working pressure angle. In a numerical example it is found that the only important vibration mode for the gear contact is the one where the gear tooth deformation is dominant. The bearing force variation, however, will be much more affected by the other vibration modes. The influence of the friction force is also studied. The friction has no dynamic influence on the gear contact force or on the bearing force in the gear mesh line-of-action direction. On the other hand, the changing of sliding directions in the pitch point is a source for critical oscillations of the bearings in the gear tooth frictional direction. These bearing force oscillations in the frictional direction appear unaffected by the dynamic response along the gear mesh line-of-action direction.

1. Introduction

To be able to dimension a gear set with its bearings, knowledge about the forces acting on the gear teeth and the bearings at the instantaneous speed is needed. Normally, the dimensioning is carried out by using the static forces corrected with a dynamic factor to include the influence of the velocity. The dynamic factors that are used in that kind of calculation are usually monotonically increasing functions of the velocity. A major shortcoming of using such factors is that no consideration is given to the magnitude of the velocity in relation to the natural frequencies. Therefore, of course, it is interesting to develop a model where the dynamic factors

*Corresponding author. Fax: +46-46-2228504.
E-mail address: lars.vedmar@mel.lth.se (L. Vedmar).

0022-460X/03/$ - see front matter
doi:10.1016/S0022-460X(03)00358-4

can be determined even close to the natural frequencies of the gear set. A lot of such models, using different kinds of approximations, have been used to describe the dynamic response in gear sets.

The gear mesh has been modelled using constant stiffness by e.g., Kahraman and Singh [1] and Andersson [2]. Others have by used a mesh stiffness calculated by using cantilever beams, for example Ichimaru and Hirano [3], Yoon and Rao [4] and Lin, et al. [5].

Vedmar and Henriksson [6] introduced a method to use the deformations of the gears to determine the variation of the gear mesh stiffness and the boundary of the action between the gears. Special care was here taken to find the true entrance and exit points of the gear contact outside the line of action. In these points the contact force should equal zero at the same time as the gear deformation is zero. In a comparative study this way of calculating the gear force was compared to that when all action was assumed to take place on the straight line of action. This study revealed the importance of using the smoother entrance and exit conditions in the analysis if the interest is to determine the dynamic gear force amplitude. In that work, however, the bearings were assumed to be stiff. By that, the bearing force will correspond to the sum of the forces in all simultaneous contact points.

In Ref. [6] a contact analysis was carried out at each time step to determine the actual time-dependent stiffness. To be able to use the finite element method in such calculations an approach was used where the non-linear behaviour close to the contact could be separated from the linear behaviour in the rest of the gear material. A similar approach has been used by Parker et al. [7]. They used a semi-analytical model near the tooth surface and a finite element solution away from the tooth surface. The dynamic mesh forces were then calculated by using a detailed contact analysis at each time step as the gears roll through the mesh. The authors did not, however, reveal how they manage to handle the singularity in the entrance and exit points of the gear contacts. Further, the support is rigid and the response is purely gear rotation.

If the interest is directed more to the sound generated by the gears than just to the dimensioning forces, the bearing force variations get interesting as it is through the bearings that sound will propagate from the gear set. By that, a model ought to admit the bearings to deform. Many researchers have treated gear dynamics with elastic bearings, for instance Kahraman and Singh [8,9] and Belnikolovsky et al. [10]. No one seems, however, to have used the deformations of the gears to determine the gear mesh stiffness and the path of contact in a combination with elastic bearings.

Recent reports described friction as a source of dynamic excitations. On the basis of performed experiments, Hochmann and Houser [11] suggested that friction can produce bearing forces comparable to the ones generated by the transmission error excitations, especially at low and medium speeds. Also experiments carried out by Velex and Cahouet [12] showed that the gear friction is crucial for the bearing forces, but only at low or medium speeds. Furthermore, the transmission error seemed to be less sensitive to the gear friction than the bearing forces were. This can explain why the friction in Ref. [6], where the bearings were stiff, did not give any dynamic effect. To be able to explain the influence of the friction on the dynamics, the system studied must have some degree of freedom in the frictional direction. This could be achieved by modelling the bearings as elastic.

Vaishya and Singh [13] have studied the effect of friction-induced non-linearity in gear dynamics. The effect of including the vibratory component of the velocity when determining the sliding velocity was compared to when the sliding velocity is determined solely from the kinematic considerations. The comparison showed a considerably reduced magnitude of vibration close to the pitch point when using the non-linear model.

The objective of this paper is to develop a method to determine the gear tooth forces and the bearing forces by using a model with elastic bearings. To properly simulate the entrance and exit of the gear tooth mesh, the gear tooth contacts should be determined taking into account the deformations of both the gears and the bearings. For this purpose the model developed in Ref. [6] will be extended to include the influence of bearing deformations. Using this kind of model makes it unnecessary to externally specify the excitation in the form of time-varying mesh stiffness or using a static transmission error input. Similar analyses are not known to the authors. In the model would also be included friction between the gear teeth in contact. This will give an opportunity to study the friction-induced dynamic effects using disturbances originating from the contact analysis performed in connection with the dynamic response.

2. Gear mesh

Two perfectly manufactured and assembled involute gears will be in mesh on the straight line which is tangent to the base cylinders of the gears if the gears are assumed to be stiff. For elastic gears, however, this is no longer the case. Especially at the beginning and at the end of the mesh the contact will take place outside the straight line. The analysis must therefore take into account the contacts which will be positioned outside the straight line to be able to correctly model the load build-up on the gear teeth. Especially important is that the force build-up over time is correct to ensure a proper dynamic response.

A gear mesh starts outside the line of action with zero force at the moment just before the tooth pair will begin to deform. In this position the pinion tooth velocity along the normal direction of the contact will be different from the gear tooth velocity. The velocity difference induces a shock, which to a great extent will influence the oscillation. The complete force build-up, from the position where the gears make contact until the position where the contact cease to exist with the force exactly equal to zero, is simulated by solving the equations of motion. By this procedure no special correction for the shock is needed; it will automatically be included in the solution.

A special mathematical problem will occur in the contacts that will arise outside the line of action. The involute flank of one of the gears will here make contact with the tip corner of the other gear. This gives a singularity in the calculation of the deformation, as the corner has a zero radius of curvature. To solve this problem, the gear teeth are assumed to have somewhat rounded-out corners, giving the radius of curvature $r > 0$.

To be able to determine the forces in the gear mesh, a relation between the forces and the deformations is needed. Here the finite element method is used combined with an analytical expression by which the deformation closest to the contact is calculated. The deformation in the gear contact can in every moment be calculated when the positions of the two gears are known. These positions are given by the angles Γ_p and Γ_g. The contact between the gear teeth can take place between two involute flanks or between one involute flank and one rounded-out corner. First, study the contact between two involute flanks. When the gears are unloaded and in contact in the pitch point the angular positions are defined to be $\Gamma_p = \Gamma_g = 0$, see Fig. 1. From this position the gears are turned the angles Γ_p and Γ_g with an assumed load which, due to bearing

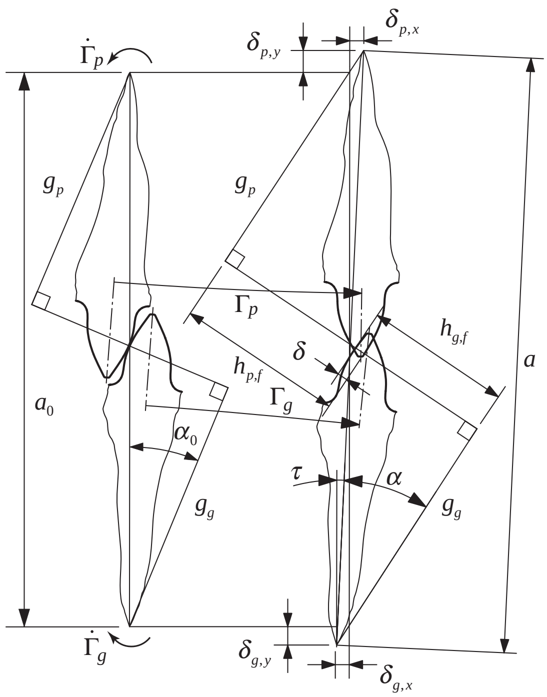

Fig. 1. Involute-involute contact.

deformations, will change the centre distance from a_0 to a at the same time as the line between the gear centres is turned an angle τ. Here

$$a = \sqrt{(\delta_{p,x} + \delta_{g,x})^2 + (a_0 + \delta_{p,y} + \delta_{g,y})^2}, \tag{1}$$

$$\sin\tau = \frac{\delta_{p,x} + \delta_{g,x}}{a}. \tag{2}$$

The gear deformation δ is shown in Fig. 1 as an overlap between two undeformed gear teeth. Using the characteristics of the involute profile gives

$$h_{p,f} = g_p\,(\tan\alpha_0 + \Gamma_p + \alpha + \tau - \alpha_0), \tag{3}$$

$$h_{g,f} = g_g\,(\tan\alpha_0 - \Gamma_g + \alpha + \tau - \alpha_0), \tag{4}$$

where

$$\cos\alpha = \frac{g_p + g_g}{a}. \tag{5}$$

The deformation will be

$$\delta = h_{p,f} + h_{g,f} - (g_p + g_g)\tan\alpha. \tag{6}$$

Instead of contact between the involute flanks of the two contacting gear teeth, the contact can take place between the involute flank on one of the gear tooth and the rounded-out corner on a tooth of the other gear. Fig. 2 shows a contact between the involute flank of the gear and the

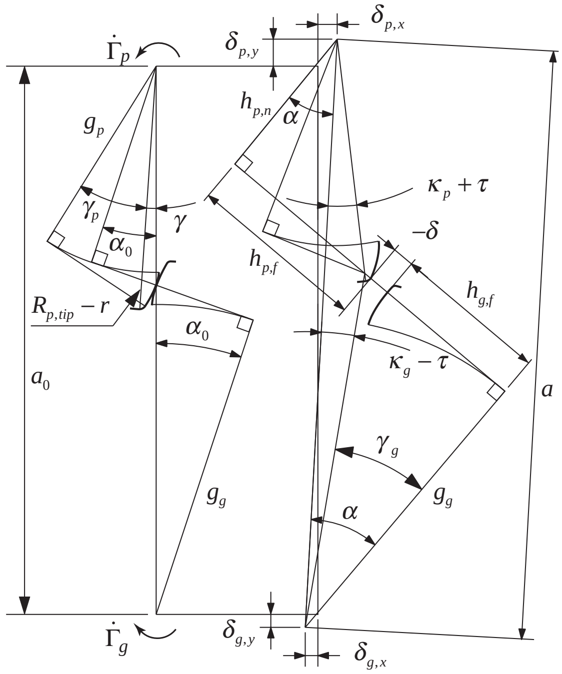

Fig. 2. Contact between involute and rounded-out corner.

rounded-out corner of the pinion. When the gears are unloaded, the centre point of the tip rounding relative to a line between the gear centres is given by the angle γ. With

$$\cos\gamma_p = \frac{g_p}{R_{p,tip} - r}, \tag{7}$$

this angle becomes

$$\gamma = \tan\gamma_p + \frac{r}{g_p} - \tan\alpha_0 + \alpha_0 - \gamma_p. \tag{8}$$

When loaded, the pinion and the gear turn the angles Γ_p and Γ_g, respectively. The position of the centre point of the tip rounding is in this position described by the angles κ_p and κ_g, for which

$$\kappa_p = \Gamma_p - \gamma, \tag{9}$$

$$\tan(\kappa_g - \tau) = \frac{(R_{p,tip} - r)\sin(\kappa_p + \tau)}{a - (R_{p,tip} - r)\cos(\kappa_p + \tau)}. \tag{10}$$

The position of the centre point of the tip rounding of the pinion can also be described by the angle γ_g; see Fig. 2. This angle can now be determined from

$$\cos\gamma_g = \frac{g_g}{\sqrt{(R_{p,tip} - r)^2\sin^2(\kappa_p + \tau) + (a - (R_{p,tip} - r)\cos(\kappa_p + \tau))^2}}. \tag{11}$$

The contact normal has the slope

$$\alpha = \kappa_g + \gamma_g - \tau, \tag{12}$$

and the lever arms for the normal force in the contact point are

$$h_{g,n} = g_g, \tag{13}$$

$$h_{p,n} = a\cos\alpha - h_{g,n}. \tag{14}$$

The overlap δ, which corresponds to the deformation in the contact point, is

$$\delta = g_g\,(\gamma_g + \kappa_g + \tan\alpha_0 - \alpha_0 - \Gamma_g - \tan\gamma_g) + r, \tag{15}$$

and the lever arms for the friction forces in the contact point are

$$h_{g,f} = g_g \tan\gamma_g - r + \delta, \tag{16}$$

$$h_{p,f} = h_{p,n}\tan(\alpha + \kappa_p + \tau) + r. \tag{17}$$

The last possibility of contact is between the involute flank of the pinion and the tip rounding of the gear. The deformation and the lever arms for this case can be obtained by shifting the notations p and g in Eqs. (7)–(17) at the same time as the direction of the rotation is shifted ($\Gamma \rightarrow -\Gamma$).

3. Analysis

The transmission which will be analyzed is shown in Fig. 3. The gear set is coupled to external systems, which are reduced to one stiffness and one inertia at each side of the gear set. The gears are mounted on linear elastic bearings with the stiffnesses c_p and c_g while the external inertias are mounted on stiff bearings.

The transmission is driven by the torque M_{drive} and is braked by the torque M_{brake}. Loading the parts will, of course, give rise to elastic deformations. Also resisting forces due to the deformation velocity will however occur. This damping is assumed to be viscous, which implies that the torque

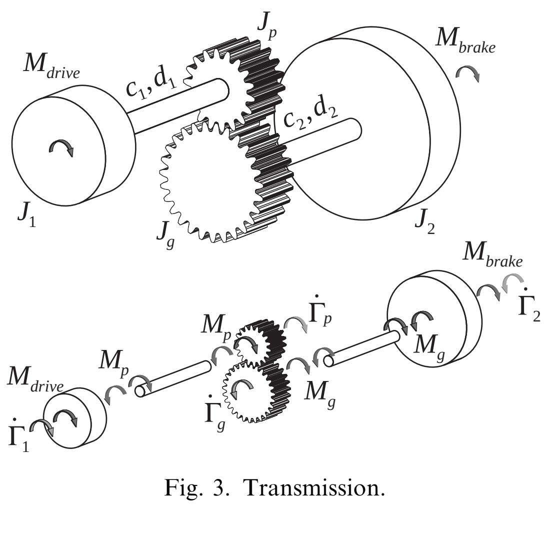

Fig. 3. Transmission.

on the gears can be expressed as

$$M_p = c_1\,(\Gamma_1 - \Gamma_p) + d_1\,(\dot{\Gamma}_1 - \dot{\Gamma}_p), \tag{18}$$

$$M_g = c_2\,(\Gamma_g - \Gamma_2) + d_2\,(\dot{\Gamma}_g - \dot{\Gamma}_2). \tag{19}$$

An arbitrary contact between the gears is shown in Fig. 4, where the deformations of the bearings are $\delta_{p,x}$, $\delta_{p,y}$, $\delta_{g,x}$, and $\delta_{g,y}$. The forces in the contact depend on the elastic deformation, the friction between the gear teeth, and the damping due to the deformation velocity. The direction of the friction force and the damping force are dependent of the velocity. The relative velocities between the gear teeth in the normal direction, and in a direction perpendicular to that, are

$$\begin{aligned}\Delta v_n = {} & \dot{\Gamma}_p h_{p,n} + \dot{\delta}_{p,x} \cos(\alpha+\tau) - \dot{\delta}_{p,y} \sin(\alpha+\tau) \\ & - \dot{\Gamma}_g h_{g,n} + \dot{\delta}_{g,x} \cos(\alpha+\tau) - \dot{\delta}_{g,y} \sin(\alpha+\tau),\end{aligned} \tag{20}$$

$$\begin{aligned}\Delta v_f = {} & \dot{\Gamma}_g h_{g,f} - \dot{\delta}_{g,x} \sin(\alpha+\tau) - \dot{\delta}_{g,y} \cos(\alpha+\tau) \\ & - \dot{\Gamma}_p h_{p,f} - \dot{\delta}_{p,x} \sin(\alpha+\tau) - \dot{\delta}_{p,y} \cos(\alpha+\tau).\end{aligned} \tag{21}$$

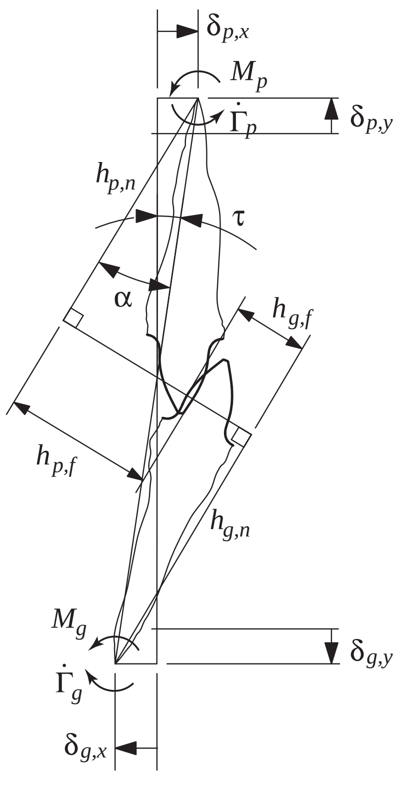

Fig. 4. Gear contact.

The equations of motion can now be formulated as

$$J_1\ddot{\Gamma}_1 = M_{drive} - M_p, \tag{22}$$

$$J_p\ddot{\Gamma}_p = M_p - \sum_i\left((F_i + d\Delta v_{n,i})\,h_{p,n,i} - \mu\frac{\Delta v_{f,i}}{|\Delta v_{f,i}|}F_ih_{p,f,i}\right), \tag{23}$$

$$J_g\ddot{\Gamma}_g = -M_g + \sum_i\left((F_i + d\Delta v_{n,i})\,h_{g,n,i} - \mu\frac{\Delta v_{f,i}}{|\Delta v_{f,i}|}F_ih_{g,f,i}\right), \tag{24}$$

$$J_2\ddot{\Gamma}_2 = M_g - M_{brake}, \tag{25}$$

$$m_p\ddot{\delta}_{p,x} = \sum_i\left(-F_i\cos(\alpha_i + \tau) + \mu F_i\frac{\Delta v_{f,i}}{|\Delta v_{f,i}|}\sin(\alpha_i + \tau)\right) - c_p\delta_{p,x} - d_p\dot{\delta}_{p,x}, \tag{26}$$

$$m_p\ddot{\delta}_{p,y} = \sum_i\left(F_i\sin(\alpha_i + \tau) + \mu F_i\frac{\Delta v_{f,i}}{|\Delta v_{f,i}|}\cos(\alpha_i + \tau)\right) - c_p\delta_{p,y} - d_p\dot{\delta}_{p,y}, \tag{27}$$

$$m_g\ddot{\delta}_{g,x} = \sum_i\left(-F_i\cos(\alpha_i + \tau) + \mu F_i\frac{\Delta v_{f,i}}{|\Delta v_{f,i}|}\sin(\alpha_i + \tau)\right) - c_g\delta_{g,x} - d_g\dot{\delta}_{g,x}, \tag{28}$$

$$m_g\ddot{\delta}_{g,y} = \sum_i\left(F_i\sin(\alpha_i + \tau) + \mu F_i\frac{\Delta v_{f,i}}{|\Delta v_{f,i}|}\cos(\alpha_i + \tau)\right) - c_g\delta_{g,y} - d_g\dot{\delta}_{g,y}, \tag{29}$$

where the sums have been used to sum up the influence of the, possible, several simultaneous contacts.

In the equations the friction force is clearly non-linear as it depend on both the normal force and the velocity difference and this difference includes the vibratory component. The variation of μ could, according to Ref. [13], be ignored, as changes in the magnitude of the coefficient of friction are less significant when compared with effect of the reversal of sign at the pitch point. A coulomb model of the friction will therefore be used.

To be able to solve the equations of motion, these are rewritten as a system of first order equations. These are then solved by using the Runge–Kutta method. When doing this, the forces between the gear teeth are needed in every moment. These are given by the known values of the gear deformations, earlier described as an overlap δ, in every possible mesh position. The stiffness, which has to be known to be able to calculate the forces from the known deformations, is calculated by using the finite element method. In this calculation the stiffness will be calculated by using the displacement in the same point as where the resultant load on the gear tooth acts. It is therefore important to use the correct distribution of the load on the gear tooth. One way to do this, without using an unnecessary number of elements, was developed in Ref. [14] for three-dimensional helical gears and is described in Ref. [6] for the two-dimensional spur gear case. With this method the flexibilities α_p and α_g of the loaded gear tooth and of its neighbours are calculated for load positions all over the gear tooth flank. To completely describe the deformation, the non-linear deformations $u_{p,c}$ and $u_{g,c}$ representing the deformation closest to the contact point where the distribution of the force is of importance should be added to the deformation received by using the flexibilities. An analytical expression of the deformations $u_{p,c}$ and $u_{g,c}$ is used. This is the result of an integration of the deformations between the surface and a point at a certain depth for a semi-infinite plate subjected to a Hertzian distributed surface load; see Ref. [6].

With k simultaneous contacts, where the gear deformation in a certain moment is δ_i, $i = 1, 2, \ldots, k$, the normal gear forces F_i, $i = 1, 2, \ldots, k$ are determined by using the equation

$$\left\{ \begin{array}{c} u_{p,c,1}(F_1) + u_{g,c,1}(F_1) + \sum_{j=1}^{k} (\alpha_{p,1,j} + \alpha_{g,1,j}) F_j = \delta_1 \\ u_{p,c,2}(F_2) + u_{g,c,2}(F_2) + \sum_{j=1}^{k} (\alpha_{p,2,j} + \alpha_{g,2,j}) F_j = \delta_2 \\ \vdots \\ u_{p,c,k}(F_k) + u_{g,c,k}(F_k) + \sum_{j=1}^{k} (\alpha_{p,k,j} + \alpha_{g,k,j}) F_j = \delta_k \end{array} \right\}. \tag{30}$$

On account of the coupling effect between the gear teeth, there can be a displacement in a point even if this point itself is unloaded. The equation must therefore be solved to also satisfy the conditions

$$F_i \geqslant 0, \quad i = 1, 2, \ldots, k. \tag{31}$$

A flow chart of the computational procedure used when calculating the dynamic response for a specific speed is shown in Fig. 5.

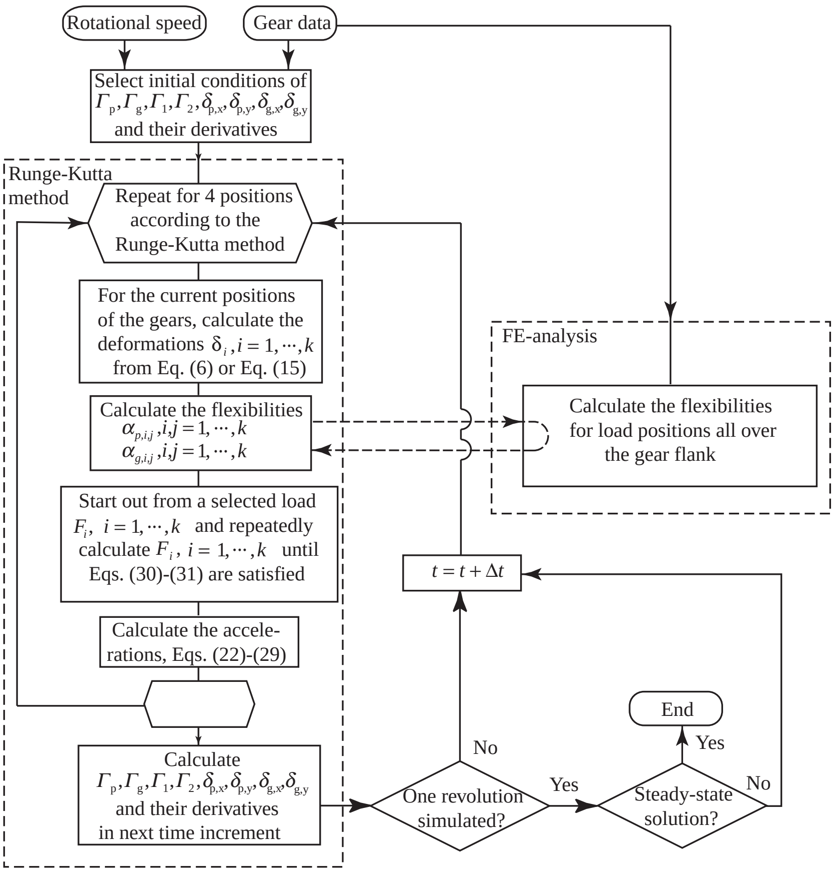

Fig. 5. Flow chart of the computational procedure.

4. Results

To actually solve the equations, a lot of numerical data are needed. Specifically, the damping coefficients are needed. In a lightly damped system, as the one studied, the damping is small enough not to significantly influence the natural frequencies. However, some amount of damping has to be present to give a steady-state solution independent of the starting conditions. Here values are chosen which gives relative damping coefficients around $0 \cdot 03$.

In Table 1, all the numerical values used in the calculations are given. The calculation gives, among others, the deformations in the gear contacts and in the bearings. With these deformations, the forces between the gear teeth in mesh and on the bearings can be calculated. Of course, the forces at for instance a start-up process can be interesting to determine, but here only a steady state solution will be given.

In Fig. 6 the normal force on a gear tooth during its mesh and the bearing forces, in and perpendicular to the unloaded mesh plane, are shown when the gears are not moving, that is statically. The two directions in which the bearing forces are given will hereinafter be called the normal direction and the frictional direction despite the fact that this is not absolutely correct in the beginning and end of the action. Here, the rounded-out corner of one gear makes contact with the involute flank of the other gear. Since the inertias of the gears do not give any contribution to the forces in this static case, the bearing force will be equal to the total gear forces, that is the sum of the forces on the teeth simultaneously in mesh. Thereby, the bearing forces will also be the same on both the pinion and the gear.

In the pitch point, the normal force on a gear tooth will, due to the change in direction of the friction force, change between the extreme values

$$F = \frac{M_{brake}}{g_g} \frac{1}{(1 \pm \mu \tan \alpha)}, \tag{32}$$

Table 1
Numerical data

Number of teeth	$z_p = z_g = 20$
Basic rack module	5 mm
Face width	25 mm
Pressure angle	20°
Theoretical contact ratio	$\varepsilon = 1.56$
Tooth tip rounding radius	$r = 0.05m$
Normal backlash	$0.0725m$
Input and output inertia	$J_1 = J_2 = 0.62$ kg m^2
Gear inertia	$J_p = J_g = 0.0019$ kg m^2
Gear mass	$m_p = m_g = 1.53$ kg
Input and output stiffness	$c_1 = c_2 = 7596$ N m
Input and output damping	$d_1 = d_2 = 0.04$ N m s
Bearing damping	$d_p = d_g = 1400$ N s/m
Gear damping	$d = 700$ N s/m
Pinion bearing stiffness	$c_p = 2 \times 10^8$ N/m
Gear bearing stiffness	$c_g = 3 \times 10^8$ N/m
Braking torque	$M_{brake} = 1000$ N m

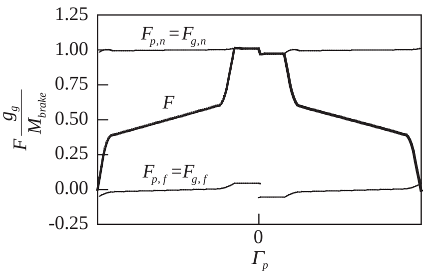

Fig. 6. Gear and bearing forces when $\mu = 0.05$ and $n_p = 0$.

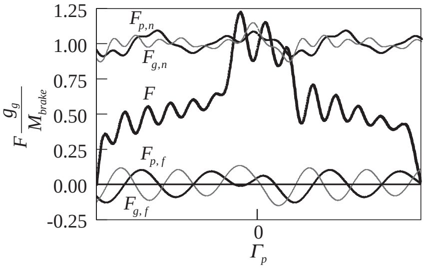

Fig. 7. Gear and bearing forces when $\mu = 0.05$ and $n_p = 2000$ r.p.m.

which implies that the normal force on the tooth will be approximately 1.019 times greater when the friction coefficient $\mu = 0.05$ compared to when the friction coefficient $\mu = 0$. When two gear teeth on each gear are simultaneously in mesh, the friction forces in the two contacts act in opposite directions and by that the bearing forces in the frictional direction will be small. When there is only one contact, the friction force will act in different directions depending on which side of the pitch point the contact will take place in. Thereby, the total friction force will at the most be 5% of the normal force on the gear tooth for the current friction coefficient $\mu = 0.05$. This gives a greater variation of the bearing force in the frictional direction than in the normal direction. However, the bearing force in the frictional direction is so small compared to the bearing force in the normal direction that the resulting bearing force mainly coincide with the bearing force in the normal direction.

Leaving the static case, the forces will now be determined when the gears rotate. In Fig. 7 the normal force on a gear tooth and the bearing forces on the two gears in the normal direction and the frictional direction are shown, when the pinion velocity $n_p = 2000$ r.p.m. Compared to the earlier static case, the inertias of the gears here give bearing forces which deviate from the total gear force. This is visible in the single pair region around the pitch point ($\Gamma_p = 0$) in Fig. 7. Like in the static case, the bearing force in the frictional direction varies a lot but also here the contribution from the friction to the resulting bearing force is very small. Since the bearings on the pinion and the gear here have different stiffnesses, the bearing forces will be different on the two bearings despite the fact that in this case the two gears are identical. The bearing forces can be interesting to know from different aspects. To find the sufficient dimension of the bearings the resulting load would be important to know. To make a judgement of how much noise the gear set generates, however, the variation of the forces is more important. This variation acts superposed a value which can be considered as the pre-tension of the bearing. The level of this pre-tension is, from a noise perspective, only interesting if it influences the stiffness of the bearing on account of its potential non-linear characteristic. Here, where the bearings are supposed to be linear, the level of this pre-tension is not interesting.

It can also be interesting to know, at least approximately, the natural frequencies. Therefore, a simplified model will now be studied in order to determine these frequencies. The full model contains external inertias connected to the gear set with angular springs. These external inertias induce two natural frequencies that, for the current numerical values, are considerable lower than the other natural frequencies. The external inertias can therefore be left out of account in this approximate calculation. This is done by assuming the velocities of the inertias to be constants which gives $M_p = M_{drive}$ and $M_g = M_{brake}$. Upon using a presumed constant gear mesh stiffness (studies of the deformation at static loading gave a mean value of approximately $c = 3 \times 10^8$ N/m) in a constant normal direction (given by the pressure angle α) and disregarding friction ($\mu = 0$) and damping ($d = d_p = d_g = 0$), the equations of motion (22)–(29) are transformed to

$$J_p \ddot{\Gamma}_p = M_{drive} - cug_p, \tag{33}$$

$$J_g \ddot{\Gamma}_g = -M_{brake} + cug_g, \tag{34}$$

$$m_p \ddot{\delta}_{p,x} = -cu\cos\alpha - c_p\delta_{p,x}, \tag{35}$$

$$m_p \ddot{\delta}_{p,y} = cu\sin\alpha - c_p\delta_{p,y}, \tag{36}$$

$$m_g \ddot{\delta}_{g,x} = -cu\cos\alpha - c_g\delta_{g,x}, \tag{37}$$

$$m_g \ddot{\delta}_{g,y} = cu\sin\alpha - c_g\delta_{g,y}. \tag{38}$$

Here $u = F/c$ is the deformation in the gear mesh. By introducing $u = \Gamma_p g_p - \Gamma_g g_g + \delta_{p,n} + \delta_{g,n}$ and the bearing deformations in the normal- and frictional directions

$$\delta_n = \delta_x\cos\alpha - \delta_y\sin\alpha, \tag{39}$$

$$\delta_f = \delta_x\sin\alpha + \delta_y\cos\alpha, \tag{40}$$

the equations of motion are transformed to

$$\begin{pmatrix} \ddot{u} \\ \ddot{\delta}_{p,n} \\ \ddot{\delta}_{g,n} \end{pmatrix} + \begin{pmatrix} c\left(\frac{g_p^2}{J_p} + \frac{g_g^2}{J_g} + \frac{1}{m_p} + \frac{1}{m_g}\right) & \frac{c_p}{m_p} & \frac{c_g}{m_g} \\ \frac{c}{m_p} & \frac{c_p}{m_p} & 0 \\ \frac{c}{m_g} & 0 & \frac{c_g}{m_g} \end{pmatrix} \begin{pmatrix} u \\ \delta_{p,n} \\ \delta_{g,n} \end{pmatrix} = \begin{pmatrix} M_{drive}\frac{g_p}{J_p} + M_{brake}\frac{g_g}{J_g} \\ 0 \\ 0 \end{pmatrix}, \tag{41}$$

$$\ddot{\delta}_{p,f} + \frac{c_p}{m_p}\delta_{p,f} = 0, \tag{42}$$

$$\ddot{\delta}_{g,f} + \frac{c_g}{m_g}\delta_{g,f} = 0. \tag{43}$$

The last two equations give two natural frequencies, which are completely independent of each other. By division with the number of teeth of the pinion z_p the two critical pinion frequencies will be $\omega_{p,f} = \sqrt{c_p/m_p}\frac{1}{z_p}$ and $\omega_{g,f} = \sqrt{c_g/m_g}\frac{1}{z_p}$. The gears are in fact influenced by each other by the gear friction but this was neglected in this approximate calculation. Eq. (41) gives three natural frequencies, which describe the oscillation modes along the gear normal direction. These natural frequencies give, after division by z_p, the critical frequencies $\omega_{n,1}$, $\omega_{n,2}$ and $\omega_{n,3}$. These three frequencies in the gear normal direction all depend on both the gear mesh stiffness and the two bearing stiffnesses. The lowest of the three frequencies is lower than the only one received when the bearings were supposed to be stiff.

In the general case there will consequently be five different natural frequencies, where the two in the frictional direction only are present in this direction and also completely independent of the gear mesh stiffness. If for some reason $\omega_{p,f} = \omega_{g,f}$, this frequency would also be found as one of the frequencies in the normal direction. By that, there would be no natural frequency in the frictional direction which was not present in the normal direction.

This approximate calculation ends up with the numerical values $\omega_{n,1} = 474$ rad/s, $\omega_{n,2} = 654$ rad/s, $\omega_{n,3} = 1695$ rad/s, $\omega_{p,f} = 571$ rad/s, and $\omega_{g,f} = 700$ rad/s.

If the bearings are assumed to be stiff, these natural frequencies will reduce to only one. This frequency is due to torsional oscillation in the normal direction and the numerical value, after division by the number of teeth, is $\omega_{n,0} = 1315$ rad/s.

Now leaving the approximate calculation of the natural frequencies, the variation of the bearing forces have been calculated for the pinion speed $600 \leqslant n_p \leqslant 7000$ r.p.m. for the current gear set by using the model presented in previous sections. In contrast to the approximate calculation of the natural frequencies, this analysis takes into account (a) the variation of the gear mesh stiffness through the mesh, (b) the gear stiffness dependency of the force on the actual gear tooth and also of the force on the potentially simultaneous neighbour tooth, (c) the path of contact calculated at the basis of the deformation of the gear teeth, (d) the external systems co-operating with the gear set, (e) the influence of friction and damping in the gear mesh.

In Figs. 8 and 9 the peak-to-peak bearing forces in the normal direction on the pinion and the gear, respectively, are shown. The two natural frequencies inside the velocity interval used in the calculation are clearly visible. On account of the parametric excitation, that is the variation of the gear mesh stiffness during the mesh, large variations are also received at integer fractions of the natural frequencies. Noticeably in Figs. 8 and 9 the peaks with the increased values of the force coincide well with the natural frequencies calculated by using the approximate model. It is obvious that if the interest is restricted to determine the frequencies where the forces are large, a rough model of the mesh stiffness variation will do. On the other hand, the modelling of how to start the mesh has a considerable influence on the size of the force, so in an amplitude point of view it is important to correctly describe the true mesh.

In the same way as in Figs. 8 and 9, the peak-to-peak bearing forces on the pinion and the gear are shown in Figs. 10 and 11, but now in the frictional direction. Increased peak-to-peak values are here found at the natural frequencies of the pinion and the gear in the frictional direction, $\omega_{p,f}$ and $\omega_{g,f}$, and at fractions of these frequencies. However, these fractions do not occur due to parametric excitations, as the bearing stiffness is supposed to be constant. Instead, it is the variation of the total friction force in the gear mesh that is crucial. This variation depends on the

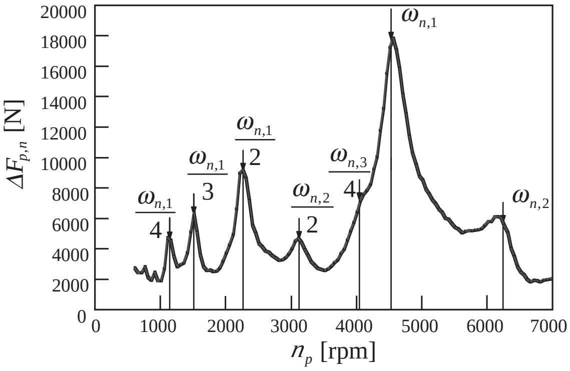

Fig. 8. Peak-to-peak bearing forces at the pinion in the normal direction when $\mu = 0.05$.

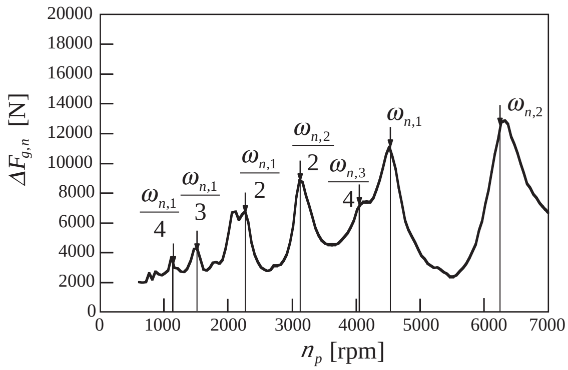

Fig. 9. Peak-to-peak bearing forces at the gear in the normal direction when $\mu = 0.05$.

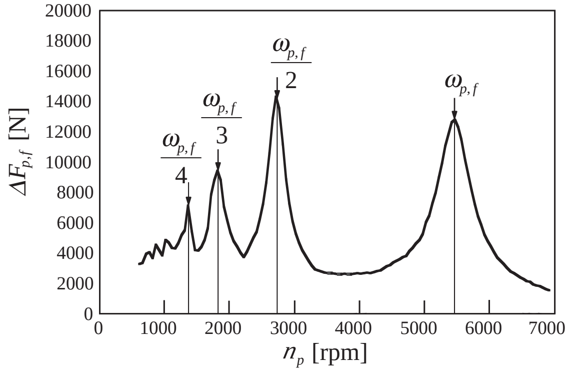

Fig. 10. Peak-to-peak bearing forces at the pinion in the frictional direction when $\mu = 0.05$.

normal force in the gear contact, which depends on the parametric excitation in the normal plane. To a great extent, however, the variation of the friction force depends on the change of sliding direction in the pitch point. The static bearing force in the frictional direction, shown in Fig. 6,

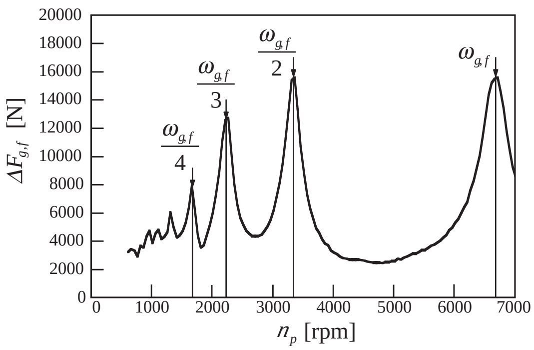

Fig. 11. Peak-to-peak bearing forces at the gear in the frictional direction when $\mu = 0.05$.

expanded in a Fourier series becomes

$$F_{p,f} = F_{g,f} = \sum_{j=1}^{\infty} b_j \sin jz_p \frac{\omega_p \pi}{30} t. \tag{44}$$

Upon using this force as the excitation of the oscillations of the bearings in the frictional direction, the equations of motion become

$$\begin{aligned} m_p\ddot{\delta}_{p,f} + d_p\dot{\delta}_{p,f} + c_p\delta_{p,f} &= \sum_{j=1}^{\infty} b_j \sin jz_p \frac{\omega_p \pi}{30} t, \\ m_g\ddot{\delta}_{g,f} + d_g\dot{\delta}_{g,f} + c_g\delta_{g,f} &= \sum_{j=1}^{\infty} b_j \sin jz_p \frac{\omega_p \pi}{30} t. \end{aligned} \tag{45}$$

From these equations, the displacements of the bearings at the critical frequencies $\omega_{p,f}/i$ and $\omega_{g,f}/i$ are

$$\begin{aligned} \delta_{p,f} &= \sum_{j=1}^{\infty} \frac{c_p\,(1-\frac{j^2}{i^2}) \sin \frac{j}{i}\sqrt{\frac{c_p}{m_p}}t - d_p\frac{j}{i}\sqrt{\frac{c_p}{m_p}} \cos \frac{j}{i}\sqrt{\frac{c_p}{m_p}}t}{c_p^2(1-\frac{j^2}{i^2})^2 + (d_p\frac{j}{i}\sqrt{\frac{c_p}{m_p}})^2} b_j, \\ \delta_{g,f} &= \sum_{j=1}^{\infty} \frac{c_g\,(1-\frac{j^2}{i^2}) \sin \frac{j}{i}\sqrt{\frac{c_g}{m_g}}t - d_g\frac{j}{i}\sqrt{\frac{c_g}{m_g}} \cos \frac{j}{i}\sqrt{\frac{c_g}{m_g}}t}{c_g^2(1-\frac{j^2}{i^2})^2 + (d_g\frac{j}{i}\sqrt{\frac{c_g}{m_g}})^2} b_j. \end{aligned} \tag{46}$$

The peak-to-peak bearing forces in the frictional direction for $i = 1, 2, 3,$ and 4 now become

$$\begin{aligned} \Delta F_{p,f} &= c_p\,(\delta_{p,f,max} - \delta_{p,f,min}) = (12300\ \text{N}, 12900\ \text{N}, 11400\ \text{N}, 7900\ \text{N}), \\ \Delta F_{g,f} &= c_g\,(\delta_{g,f,max} - \delta_{g,f,min}) = (15000\ \text{N}, 15500\ \text{N}, 13600\ \text{N}, 9200\ \text{N}). \end{aligned} \tag{47}$$

To obtain these values at least 5 terms in the sums are required. The numerical values in Eq. (47) are close to the peak values shown in Figs. 10 and 11. This means that using the static forces as excitation in this simple model will give nearly the same bearing force oscillation in the frictional direction as in the fully dynamic analysis. Thereby, it can be concluded that the bearing force oscillations in the frictional direction are rather independent of the dynamic response in the normal direction.

Now, assume for a moment that the bearings are stiff. In such a case the bearing forces of the pinion and the gear are identical. Furthermore, the bearing force is the sum of the all the simultaneous gear contact forces. In Fig. 12, the peak-to-peak bearing force in the normal- and the frictional directions for this case with stiff bearings is shown. Compared to the case with elastic bearings, the normal bearing force changes due to the changed number of natural frequencies in this direction. The really dramatic change is however found in the frictional direction. From nearly a constant value, the introduction of the elastic bearings gives resonance peaks at the natural frequencies in the frictional direction.

As the excitation in the frictional direction is dependent of the friction, the influence of the friction coefficient in the gear mesh will also be studied. In Fig. 13 the gear normal force is shown when $\mu = 0$ and 0.05. The force level is influenced by the friction but this does not depend considerably on any dynamic effects. This can be concluded by comparing the curve calculated with friction taken into account with the frictionless case corrected by the static increase from

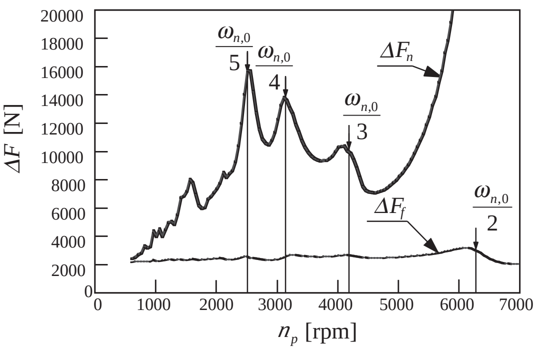

Fig. 12. Peak-to-peak bearing forces for stiff bearings.

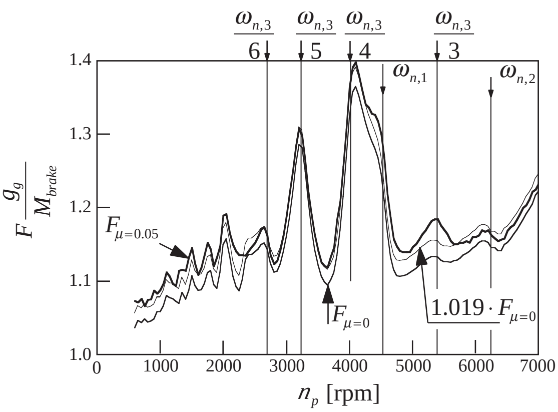

Fig. 13. Gear tooth normal forces.

Eq. (32). The two curves are very close to each other; it is only at the third fraction of the highest natural frequency that any significant difference can be observed.

In the case studied, the stiffness of the bearings are less than the gear mesh stiffness. This gives a dominating gear deformation at the oscillation mode which belongs to the natural frequency $\omega_{n,3}$. The normal gear force, shown in Fig. 13, will then increase at fractions of this frequency. The influence on the gear force amplitude at the other natural frequencies, and fractions of them, is weak.

In Ref. [6] the gear contact force was calculated assuming the bearings to be stiff. The gear contact force in that case showed increased values at the frequency $\omega_{n,0}$ and integer fractions of this frequency. As here $\omega_{n,0} < \omega_{n,3}$, the gear force will show increased values at higher speeds when taking into account the elasticity of the bearings compared to the stiff bearing case. The number of visible peaks are however unchanged.

In Fig. 14 the peak-to-peak bearing force in the normal direction is shown when the friction coefficient $\mu = 0$. A comparison of Figs. 8 and 14, in which $\mu = 0.05$ in the first and $\mu = 0$ in the latter, shows a somewhat greater force variation when the friction is taken into account. This would imply that it is possible to make a more silent gear if the friction could be decreased but the effect is marginal. However, if the friction dependency of the force variation in the frictional direction is studied the difference is much more pronounced. In Fig. 15 the peak-to-peak bearing force in the frictional direction when $\mu = 0$ is shown. Apparently, the peak-to-peak value is small,

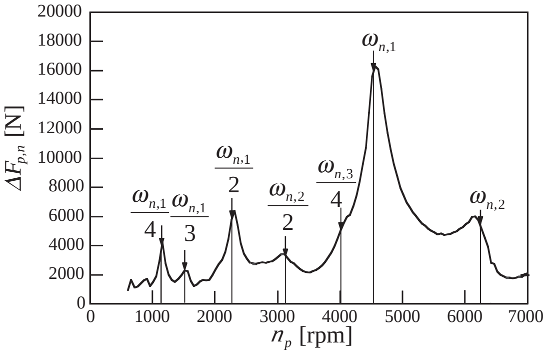

Fig. 14. Peak-to-peak bearing forces at the pinion in the normal direction when $\mu = 0$.

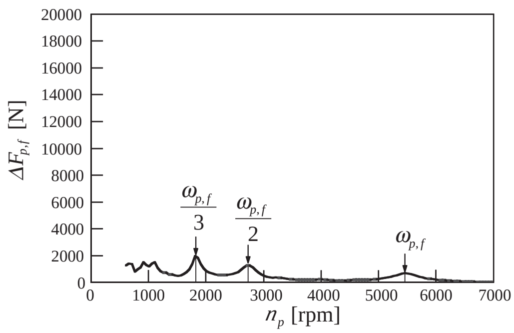

Fig. 15. Peak-to-peak bearing forces at the pinion in the frictional direction when $\mu = 0$.

less surprisingly since the exciting friction force is not present. The reason why any variation at all exists is because the gear normal force has a non-zero component in the frictional direction at the beginning and at the end of the mesh. In these regions, the rounded-out corner of the pinion or the gear makes contact with the involute flank of the co-operating gear. The magnitude is, however, small which makes the peak-to-peak bearing force in the frictional direction almost solely dependent on the friction. Despite the fact that the friction has only marginal effects on the bearing forces in the gear normal direction it may consequently have a considerable effect on the peak-to-peak bearing force in the frictional direction. Decreasing the friction in the gear mesh can decrease this variation.

5. Conclusion

The dynamic forces in the gear contact and on the bearings have been calculated for different speeds of the gears. In this calculation, account has been taken to the gear stiffness variation in the gear mesh, the successive loading and unloading of the gear teeth, the friction and the damping in the gear mesh, and the stiffness of the bearings.

Taking into account the elasticity of the bearings will, of course, increase the number of natural frequencies compared to when the bearings are assumed to be stiff. Two additional frequencies will appear in both the normal- and the frictional direction of the gear contact. The frequencies in the frictional direction are dynamically uncoupled to each other while the ones in the normal direction are coupled through the gear contact. Thereby, the natural frequencies present when taking into account the elasticity of the bearings will all be different to the frequencies present when the bearings are assumed to be stiff.

As expected, the gear force increases at fractions of the natural frequencies that belongs to the oscillation mode where the gear deformation is dominating. The influence on the gear force at other frequencies is, however, weak. Elastic bearings will therefore influence the gear normal force by increasing the resonance speed but not significantly give more resonance speeds.

When assuming the bearing to be stiff, the bearing force in the normal direction is increased at integer fractions of the natural frequency. In the frictional direction, however, the bearing load is almost at a constant level. By that, there will be no dynamic effect in this direction. With elastic bearings, the normal direction bearing force is increased at integer fractions of all natural frequencies belonging to oscillations in the normal direction. This means that there will be parametric excitations in all of these modes. In the frictional direction, elastic bearings leads to increased bearing forces at the natural frequencies of each gear and integer fractions of them. Here the friction in the gear contact manages to excite oscillations in the bearings in the frictional direction at natural frequencies that cannot be found in the normal direction. By that, the friction is able to excite oscillations in the bearings in spite of the fact that the friction in other respects does not give any considerable dynamic effect. A condition for this is however the elastic bearings. The friction itself give small dynamic effects on the gear normal force and on the bearing force in the normal direction.

The results from the calculations confirm the result from Refs. [11,12] that the friction can produce bearing forces comparable to the ones generated by the transmission error excitations This is however not restricted to specifically low and medium speeds, it depends on the natural frequencies in the frictional direction. These are independent of the dynamic response in the normal-direction and the transmissions error excitations. Further comparisons to the results from Refs. [11,12] are however difficult to make as in these reports the forces are measured in directions which are not the true normal- and frictional direction. By that the resulting force is a mix of the forces in these two directions.

Acknowledgements

This work was supported by the Swedish Research Council for Engineering Sciences (TFR).

Appendix. Nomenclature

a	centre distance (m)
b	Fourier coefficient (N)
c	stiffness (N m, N/m)
d	damping coefficient (N m s, N m/s)
F	force (N)
g	base cylinder radius (m)
h	lever arm (m)
i	number (dimensionless)
J	mass moment of inertia (kg m^2)
j	number (dimensionless)
k	number of contact points (dimensionless)
M	torque (N m)
m	mass (kg)
n	angular velocity (r.p.m.)
R, r	radius, radius of curvature (m)
u	displacement (m)
z	number of teeth (dimensionless)
α	pressure angle, flexibility (rad, m/N)
δ	gear teeth overlap, bearing deformation (m)
Δv	relative velocity (m/s)
ε	theoretical contact ratio (dimensionless)
Γ	rotational angle (rad)
γ, κ, τ	angle (rad)
μ	friction coefficient (dimensionless)
ω	angular frequency (rad/s)

Subscripts

0	unloaded, stiff bearings
1	input

2	output
c	contact
f	frictional
g	gear
n	normal
p	pinion

References

[1] A. Kahraman, R. Singh, Non-linear dynamics of a spur gear pair, Journal of Sound and Vibration 142 (1990) 49–75.

[2] A. Andersson, An analytical study of the effect of the contact ratio on the spur gear dynamic response, American Society of Mechanical Engineers, Journal of Mechanical Design 122 (2000) 508–514.

[3] K. Ichimaru, F. Hirano, Dynamic behavior of heavy-loaded spur gears, Transactions of American Society of Mechanical Engineers, Journal of Engineering for Industry (1974) 373–381.

[4] K.Y. Yoon, S.S. Rao, Dynamic load analysis of spur gears using a new tooth profile, American Society of Mechanical Engineers, Journal of Mechanical Design 118 (1996) 1–6.

[5] H.-H. Lin, R.L. Huston, J.J. Coy, On dynamic loads in parallel shaft transmissions: Part 1—modelling and analysis, Transactions of American Society of Mechanical Engineers, Journal of Mechanisms, Transmissions, and Automation in Design 110 (1988) 221–225.

[6] L. Vedmar, B. Henriksson, A general approach for determining dynamic forces in spur gears, American Society of Mechanical Engineers, Journal of Mechanical Design 120 (1998) 593–598.

[7] R.G. Parker, S.M. Vijayakar, T.B. Imajo, Non-linear dynamic response of a spur gear pair: modelling and experimental comparisons, Journal of Sound and Vibration 237 (3) (2000) 435–455.

[8] A. Kahraman, R. Singh, Error associated with a reduced order linear model of a spur gear pair, Journal of Sound and Vibration 149 (1991) 495–498.

[9] A. Kahraman, R. Singh, Non-linear dynamics of a geared rotor-bearing system with multiple clearances, Journal of Sound and Vibration 144 (1990) 469–506.

[10] B.G. Belnikolovsky, B.I. Cheshankov, B.A. Abuid, Effect of meshing parameters on the dynamic loads of a mechanism with spur gears, Dynamics and Vibration of Time-Varying Systems and Structures, in: S.C. Sinha, R.H. Evan-Iwanoski (Eds.), 14th ASME Conference on Mechanical Vibration and Noise, DE 56, American Society of Mechanical Engineers, New York, 1993, pp. 187–193.

[11] D. Hochmann, D. Houser, Friction forces as a dynamic excitation source in involute spur and helical gearing, Proceedings of the Eighth American Society of Mechanical Engineers, International Power Transmission and Gearing Conference, DETC2000/PTG-14429, 10–13 September, Baltimore, MD, 2000.

[12] P. Velex, V. Cahouet, Experimental and numerical investigations on the influence of tooth friction in spur and helical gear dynamics, American Society of Mechanical Engineers, Journal of Mechanical Design 122 (2000) 515–522.

[13] M. Vaishya, R. Singh, Sliding friction-induced non-linearity and parametric effects in gear dynamics, Journal of Sound and Vibration 248 (4) (2001) 671–694.

[14] L. Vedmar, On the design of external involute helical gears, Transactions of the Machine Elements Division, Lund, Sweden, 1981.